

## Mixed-metal cluster chemistry 25

Mixed ligand derivatives of  $\text{MoIr}_3(\mu\text{-CO})_3(\text{CO})_8(\eta\text{-C}_5\text{R}_5)$  ( $\text{R} = \text{H}, \text{Me}$ ) and  $\text{Mo}_2\text{Ir}_2(\mu\text{-CO})_3(\text{CO})_7(\eta\text{-C}_5\text{H}_5)_2$ ; X-ray crystal structures of  $\text{MoIr}_3(\mu\text{-CO})_3(\text{CO})_6(\text{PPh}_3)_2(\eta\text{-C}_5\text{Me}_5)$  and  $\text{Mo}_2\text{Ir}_2(\mu_4\text{-}\eta^2\text{-PhC}_2\text{Ph})(\mu\text{-CO})_4(\text{CNBu}^t)(\text{CO})_3(\eta\text{-C}_5\text{H}_5)_2^{\star}$ Alistair J. Usher<sup>a</sup>, Mark G. Humphrey<sup>a,\*</sup>, Anthony C. Willis<sup>b</sup><sup>a</sup> Department of Chemistry, Australian National University, Canberra ACT 0200, Australia<sup>b</sup> Research School of Chemistry, Australian National University, Canberra ACT 0200, Australia

Received 31 March 2003; received in revised form 8 July 2003; accepted 14 July 2003

## Abstract

Reactions of  $\text{MoIr}_3(\mu\text{-CO})_3(\text{CO})_8(\eta\text{-C}_5\text{Me}_5)$  (**1**) with stoichiometric amounts of the isocyanide  $\text{Bu}^t\text{NC}$  afford the ligand substituted clusters  $\text{MoIr}_3(\mu\text{-CO})_3(\text{CNBu}^t)_n(\text{CO})_{8-n}(\eta\text{-C}_5\text{Me}_5)$  ( $n = 1$  (**2**), 2 (**3**), 3 (**4**)) in fair to good yields (13–58%). In contrast, **1** reacts with  $\text{PPh}_3$  to afford a single unexpected product, namely  $\text{MoIr}_3(\mu\text{-CO})_3(\text{CO})_6(\text{PPh}_3)_2(\eta\text{-C}_5\text{Me}_5)$  (**5**). A single-crystal X-ray study of **5** reveals that the phosphines occupy coordination sites adjacent to the plane of bridging carbonyls in a radial–radial–axial conformation previously unobserved in structural studies of molybdenum–tri-iridium or tungsten–tri-iridium clusters. Reactions of  $\text{Mo}_2\text{Ir}_2(\mu\text{-CO})_3(\text{CO})_7(\eta\text{-C}_5\text{H}_5)_2$  (**6**) with  $\text{Bu}^t\text{NC}$  or diphenylacetylene proceed cleanly in high yield to afford  $\text{Mo}_2\text{Ir}_2(\mu\text{-CO})_2(\text{CNBu}^t)_2(\text{CO})_6(\eta\text{-C}_5\text{H}_5)_2$  (**7**) or  $\text{Mo}_2\text{Ir}_2(\mu_4\text{-}\eta^2\text{-PhC}_2\text{Ph})(\mu\text{-CO})_4(\text{CO})_4(\eta\text{-C}_5\text{H}_5)_2$  (**8**), respectively; reacting **7** with diphenylacetylene or **8** with  $\text{Bu}^t\text{NC}$  results in a more complex mixture of products from which  $\text{Mo}_2\text{Ir}_2(\mu_4\text{-}\eta^2\text{-PhC}_2\text{Ph})(\mu\text{-CO})_4(\text{CNBu}^t)(\text{CO})_3(\eta\text{-C}_5\text{H}_5)_2$  (**9**) can be isolated in low yield.

© 2003 Elsevier B.V. All rights reserved.

Keywords: Molybdenum; Iridium; Carbonyl; Isocyanide; Phosphine; Pentamethylcyclopentadienyl; Cluster

## 1. Introduction

Clusters containing disparate metals ('very mixed'—metal clusters [2]) are of interest as sites for unusual substrate activation and as species at which to examine metallo-, bond- and site-selectivity. We have a long-standing interest in the chemistry of tetrahedral Group 6–iridium clusters, having reported phosphine, phos-

phite, isocyanide and alkyne chemistry of these clusters: see, for example, Refs. [3–7].

Most of our earlier reports have considered cyclopentadienyl-containing clusters  $\text{M}\text{Ir}_3(\mu\text{-CO})_n(\text{CO})_{11-n}(\eta\text{-C}_5\text{H}_5)$  or  $\text{M}_2\text{Ir}_2(\mu\text{-CO})_n(\text{CO})_{10-n}(\eta\text{-C}_5\text{H}_5)_2$  ( $\text{M} = \text{Mo}, n = 3$ ;  $\text{M} = \text{W}, n = 0$ ). Increasing both electron richness and steric crowding at the cluster core might be expected to influence subsequent chemistry. To probe this possibility, we have examined the phosphine and isocyanide chemistry of  $\text{MoIr}_3(\mu\text{-CO})_3(\text{CO})_8(\eta\text{-C}_5\text{Me}_5)$  (**1**), the results from which are described herein. Also reported herein are our first attempts to prepare mixed alkyne-isocyanide adducts of Group 6–iridium clusters.

<sup>\*</sup> See Ref. [1].

\* Corresponding author. Tel.: +61-2-61252927; fax: +61-2-61250760.

E-mail address: [mark.humphrey@anu.edu.au](mailto:mark.humphrey@anu.edu.au) (M.G. Humphrey).

## 2. Results and discussion

### 2.1. Synthesis and characterization of $\text{MoIr}_3(\mu\text{-CO})_3(\text{CNBu}^t)_n(\text{CO})_{8-n}(\eta\text{-C}_5\text{Me}_5)$ ( $n = 1$ (**2**), 2 (**3**), 3 (**4**))

The reactions of  $\text{MoIr}_3(\mu\text{-CO})_3(\text{CO})_8(\eta\text{-C}_5\text{Me}_5)$  (**1**) with  $n$  equivalents of  $\text{Bu}^t\text{NC}$  ( $n = 1, 2$ ) proceed in  $\text{CH}_2\text{Cl}_2$  or THF at room temperature. Product distributions obtained are shown in Table 1. Reaction of **1** with one equivalent of  $\text{Bu}^t\text{NC}$  produces a wider product distribution than the analogous reaction of  $\text{MoIr}_3(\mu\text{-CO})_3(\text{CO})_8(\eta\text{-C}_5\text{H}_5)$  [**1**]. Reaction with two equivalents affords a mixture of  $\text{MoIr}_3(\mu\text{-CO})_3(\text{CNBu}^t)_n(\text{CO})_{8-n}(\eta\text{-C}_5\text{Me}_5)$  ( $n = 0\text{--}3$ ) roughly centred on  $n = 2$  (**3**) as the major product.

The cluster  $\text{MoIr}_3(\mu\text{-CO})_3(\text{CNBu}^t)(\text{CO})_7(\eta\text{-C}_5\text{Me}_5)$  (**2**) was characterized by IR,  $^1\text{H-NMR}$  spectroscopy, MS and satisfactory microanalysis. The complexes  $\text{MoIr}_3(\mu\text{-CO})_3(\text{CNBu}^t)_2(\text{CO})_6(\eta\text{-C}_5\text{Me}_5)$  (**3**) and  $\text{MoIr}_3(\mu\text{-CO})_3(\text{CNBu}^t)_3(\text{CO})_5(\eta\text{-C}_5\text{Me}_5)$  (**4**) were found to be unstable in solution over short periods of time and were tentatively assigned by solution IR. All IR spectra closely resemble those of their cyclopentadienyl analogues [**1**], display the expected number of bands in the  $\nu(\text{NC})$  region and contain bands corresponding to both terminal and edge bridging carbonyl ligands. The number of bands in the  $\nu(\text{CO})$  region is also consistent with the presence of isomers. The  $^1\text{H-NMR}$  spectrum of **2** shows resonances from pentamethylcyclopentadienyl and *tert*-butyl groups in the predicted ratio, and the mass spectrum shows a molecular ion at the expected  $m/z$  value followed by successive loss of all carbonyls.

### 2.2. Synthesis and characterization of $\text{MoIr}_3(\mu\text{-CO})_3(\text{CO})_6(\text{PPh}_3)_2(\eta\text{-C}_5\text{Me}_5)$ (**5**)

The reaction of **1** with one equivalent of  $\text{PPh}_3$  proceeds in  $\text{CH}_2\text{Cl}_2$  at room temperature to surprisingly give a single product,  $\text{MoIr}_3(\mu\text{-CO})_3(\text{CO})_6(\text{PPh}_3)_2(\eta\text{-C}_5\text{Me}_5)$  (**5**), in moderate yield. Reaction of **1** with half an equivalent of  $\text{PPh}_3$  also afforded **5**, and did not afford the expected mono- $\text{PPh}_3$  substituted cluster. The product **5** was characterized by solution IR,  $^1\text{H-NMR}$ , fast atom bombardment mass spectra (FABMS), a single-crystal X-ray structure determination and satis-

factory microanalysis. The IR spectrum contains  $\nu(\text{CO})$  bands in the terminal and bridging carbonyl regions and is analogous to the spectrum of  $\text{MoIr}_3(\mu\text{-CO})_3(\text{CO})_6(\text{PPh}_3)_2(\eta\text{-C}_5\text{H}_5)$  [**8**]. The number of bands in the IR spectrum is indicative of the presence of isomers in solution. The  $^1\text{H-NMR}$  spectrum of **5** contains resonances in the phenyl and methyl regions in the expected ratio. The mass spectrum contains a molecular ion at the expected  $m/z$  value and fragment ions corresponding to sequential loss of all carbonyl ligands.

### 2.3. X-ray structural study of $\text{MoIr}_3(\mu\text{-CO})_3(\text{CO})_6(\text{PPh}_3)_2(\eta\text{-C}_5\text{Me}_5)$ (**5**)

A crystal of  $\text{MoIr}_3(\mu\text{-CO})_3(\text{CO})_6(\text{PPh}_3)_2(\eta\text{-C}_5\text{Me}_5)$  (**5**) was subjected to X-ray diffraction analysis; the solid-state molecular structure and atomic labelling scheme are shown in Fig. 1 [**9**]. Relevant crystal data and structure refinement details for the structural study are collected in Table 2, while selected bond lengths and angles are listed in Table 3.

The cluster has the pseudotetrahedral framework of the precursor cluster and possesses an  $\eta\text{-C}_5\text{Me}_5$  ligand, three bridging carbonyls arranged around an  $\text{MoIr}_2$  face, six terminal carbonyl ligands and a triphenylphosphine ligand coordinated to each iridium atom in the plane of bridging carbonyls. The metal–metal and Ir–P bond distances are not unusual and intraphosphine bond lengths and angles are within the expected ranges. Metal–metal bonds bridged by carbonyl ligands tend to be slightly shorter than unbridged metal–metal bonds, a trend also observed in the precursor cluster. The unsymmetrical disposition of bridging carbonyl ligands is similar to that observed in  $\text{MoIr}_3(\mu\text{-CO})_3(\text{CO})_7(\text{PPh}_3)(\eta\text{-C}_5\text{H}_5)$  [**8**] and  $\text{WIr}_3(\mu\text{-CO})_3(\text{CO})_7(\text{PPh}_3)(\eta\text{-C}_5\text{H}_5)$  [**3**].

### 2.4. Synthesis and characterization of $\text{Mo}_2\text{Ir}_2(\mu_4\text{-}\eta^2\text{-PhC}_2\text{Ph})(\mu\text{-CO})_4(\text{CNBu}^t)(\text{CO})_3(\eta\text{-C}_5\text{H}_5)_2$ (**9**)

The reactions of  $\text{Mo}_2\text{Ir}_2(\mu\text{-CO})_3(\text{CO})_7(\eta\text{-C}_5\text{H}_5)_2$  (**6**) with  $\text{Bu}^t\text{NC}$  or  $\text{PhC}_2\text{Ph}$  proceed cleanly in high yield, affording the cluster adducts  $\text{Mo}_2\text{Ir}_2(\mu\text{-CO})_2(\text{CNBu}^t)_2(\text{CO})_6(\eta\text{-C}_5\text{H}_5)_2$  (**7**) [**1**] or  $\text{Mo}_2\text{Ir}_2(\mu_4\text{-}\eta^2\text{-PhC}_2\text{Ph})(\mu\text{-CO})_4(\text{CO})_4(\eta\text{-C}_5\text{H}_5)_2$  (**8**) [**10**], respectively. Subsequent reactions of these cluster adducts with  $\text{PhC}_2\text{Ph}$  or  $\text{CNBu}^t$ , respectively, are shown in Scheme 1.

Reaction of **7** with  $\text{PhC}_2\text{Ph}$ , under the same conditions as the aforementioned reaction of the parent cluster, produced a complex mixture of products in low yield, the major product being  $\text{Mo}_2\text{Ir}_2(\mu_4\text{-}\eta^2\text{-PhC}_2\text{Ph})(\mu\text{-CO})_4(\text{CNBu}^t)(\text{CO})_3(\eta\text{-C}_5\text{H}_5)_2$  (**9**) (17%). Similarly, reaction of **8** with  $\text{Bu}^t\text{NC}$  under the same conditions as the reaction of the parent cluster afforded a reduced yield of the intended product. The cluster **9**

Table 1  
Product distributions obtained from reactions of  $\text{Bu}^t\text{NC}$  with **1**

	Product yields (%)		
	<b>2</b>	<b>3</b>	<b>4</b>
One equivalent $\text{Bu}^t\text{NC}$	58	2	–
Two equivalents $\text{Bu}^t\text{NC}$	31	42	13

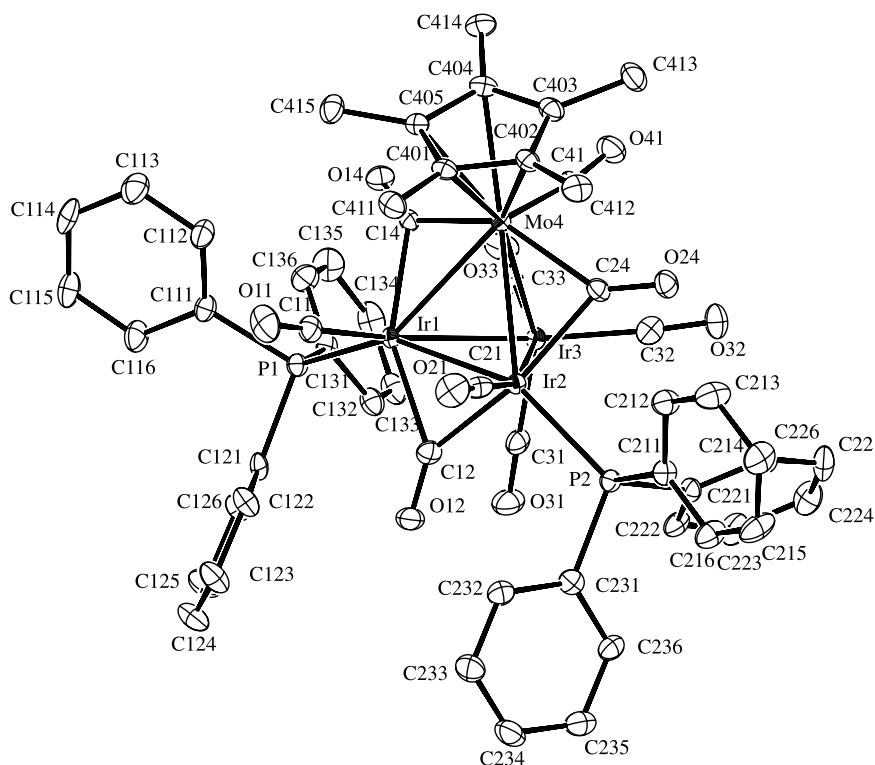


Fig. 1. ORTEP [9] plot and atomic numbering scheme for  $\text{MoIr}_3(\mu\text{-CO})_3(\text{CO})_6(\text{PPh}_3)_2(\eta\text{-C}_5\text{Me}_5)$  (**5**). Displacement ellipsoids are at the 30% probability level. Hydrogen atoms have been omitted for clarity.

was characterized by a combination of solution IR,  $^1\text{H-NMR}$  spectroscopy, FABMS, a single-crystal X-ray structural study and satisfactory microanalysis. The solution IR spectrum contains a single band in the  $\nu(\text{NC})$  region and a number of  $\nu(\text{CO})$  bands distributed through the terminal and bridging carbonyl regions. The  $^1\text{H-NMR}$  spectrum contains resonances in the phenyl, cyclopentadienyl and *tert*-butyl regions in the expected ratios, as well as a  $\text{CH}_2\text{Cl}_2$  signal corresponding to the crystallographically-verified solvent of crystallization. The mass spectrum shows a molecular ion at the expected  $m/z$  ratio and fragment ions corresponding to successive loss of seven carbonyl ligands.

Small amounts of a short-lived species were tentatively identified as  $\text{Mo}_2\text{Ir}_2(\mu_4\text{-}\eta^2\text{-PhC}_2\text{Ph})(\mu\text{-CO})_4(\text{CNBu}^t)_2(\text{CO})_2(\eta\text{-C}_5\text{H}_5)_2$  by solution IR but were only obtained as a mixture with the mono- $\text{Bu}^t\text{NC}$  substituted cluster. This complex was found to decompose rapidly to form  $\text{Mo}_2\text{Ir}_2(\mu_4\text{-}\eta^2\text{-PhC}_2\text{Ph})(\mu\text{-CO})_4(\text{CNBu}^t)(\text{CO})_3(\eta\text{-C}_5\text{H}_5)_2$  and a thick brown residue, elimination of a  $\text{Bu}^t\text{NC}$  ligand being likely to ease steric crowding around the cluster core.

### 2.5. X-ray structural study of $\text{Mo}_2\text{Ir}_2(\mu_4\text{-}\eta^2\text{-PhC}_2\text{Ph})(\mu\text{-CO})_4(\text{CNBu}^t)(\text{CO})_3(\eta\text{-C}_5\text{H}_5)_2$ (**9**)

A crystal of  $\text{Mo}_2\text{Ir}_2(\mu_4\text{-}\eta^2\text{-PhC}_2\text{Ph})(\mu\text{-CO})_4(\text{CNBu}^t)(\text{CO})_3(\eta\text{-C}_5\text{H}_5)_2$  (**9**) was subjected to X-

ray diffraction analysis; the solid-state molecular structure and atomic numbering scheme is shown in Fig. 2 [9]. Relevant crystal data and structure refinement details for the structural study are collected in Table 2, while selected bond lengths and angles are listed in Table 4.

The cluster possesses a  $\text{Mo}_2\text{Ir}_2$  core in which the metal atoms adopt a butterfly geometry: the iridium atoms form the hinge and the molybdenum atoms reside at the wingtip positions. Each molybdenum atom bears a cyclopentadienyl ring and each iridium is ligated by two terminal ligands, Ir2 by two carbonyls and Ir1 by one carbonyl and one  $\text{Bu}^t\text{NC}$  ligand, the latter lying trans to the Ir–Ir vector. The remaining carbonyls each bridge one Mo–Ir bond. The diphenylacetylene ligand bridges all four metal atoms in a  $\mu_4\text{-}\eta^2$ -manner and lies parallel to the Ir–Ir vector giving the cluster a close-octahedral  $\text{Mo}_2\text{Ir}_2\text{C}_2$  core. All metal–metal bond lengths fall within the expected ranges. Cluster **9** possesses a similar ligand disposition to the precursor **8**, the only significant difference being substitution of a carbonyl trans to the Ir–Ir bond by the  $\text{Bu}^t\text{NC}$ .

### 2.6. Discussion

Reactions of  $\text{MoIr}_3(\mu\text{-CO})_3(\text{CO})_8(\eta\text{-C}_5\text{H}_5)$  (**10**) with stoichiometric amounts of  $\text{Bu}^t\text{NC}$  afford  $\text{MoIr}_3(\mu\text{-CO})_3(\text{CNBu}^t)_n(\text{CO})_{8-n}(\eta\text{-C}_5\text{H}_5)$  ( $n = 1\text{--}3$ ), for which

Table 2  
Crystal data and structure refinement details for **5** and **9**

	<b>5</b>	<b>9</b>
Empirical formula	C <sub>55</sub> H <sub>45</sub> Ir <sub>3</sub> MoO <sub>9</sub> P <sub>2</sub> ·2(CH <sub>2</sub> Cl <sub>2</sub> )	C <sub>36</sub> H <sub>29</sub> Ir <sub>2</sub> Mo <sub>2</sub> NO <sub>7</sub> ·CH <sub>2</sub> Cl <sub>2</sub>
Formula weight	1754.37	1248.88
Temperature (K)	200	293
Colour, habit	Orange, plate	Green, needle
Crystal system	Monoclinic	Triclinic
Space group	<i>P</i> 2 <sub>1</sub> / <i>c</i>	<i>P</i> $\bar{1}$
<i>a</i> (Å)	17.8385(1)	9.9765(2)
<i>b</i> (Å)	14.4457(1)	10.5041(2)
<i>c</i> (Å)	22.3903(2)	19.3866(4)
$\alpha$ (°)	90	92.206(1)
$\beta$ (°)	90.7204(4)	100.650(1)
$\gamma$ (°)	90	108.682(1)
<i>V</i> (Å <sup>3</sup> )	5769.29(7)	1880.96(7)
<i>Z</i>	4	2
Crystal size (mm)	0.50 × 0.30 × 0.03	0.28 × 0.05 × 0.04
<i>D</i> <sub>calc</sub> (g cm <sup>-3</sup> )	2.020	2.205
$\mu$ (mm <sup>-1</sup> )	7.405	7.895
$\theta_{\max}$ (°)	27.5	27.5
<i>N</i> <sub>cell</sub>	113 480	75 270
<i>N</i> <sub>collected</sub>	113 539	37 564
<i>N</i> <sub>unique</sub>	13 185	8601
<i>N</i> <sub>obs</sub>	7481 ( <i>I</i> > 3.00σ( <i>I</i> ))	6143 ( <i>I</i> > 3.00σ( <i>I</i> ))
Absorption correction	Integration	Integration
<i>T</i> <sub>min</sub> , <i>T</i> <sub>max</sub>	0.134, 0.656	0.312, 0.750
Parameters	685	457
<i>R</i> <sup>a</sup>	0.0226	0.0296
<i>R</i> <sub>w</sub> <sup>b</sup>	0.0252	0.0328
<i>S</i>	1.07	1.05
(Δρ) <sub>min</sub> (e Å <sup>-3</sup> )	-1.24	-1.17
(Δρ) <sub>max</sub> (e Å <sup>-3</sup> )	0.98	1.37

$$^a R = \sum ||F_o| - |F_c|| / \sum |F_o|.$$

$$^b R_w = [(\sum w(|F_o| - |F_c|)^2) / \sum wF_o^2]^{1/2}.$$

the *trans*-substituted product is unstable in solution [1]. The pentamethylcyclopentadienyl-containing analogue **1** reacts with Bu<sup>t</sup>NC in the present studies to give a similar product distribution, but both the bis- and tris-substituted products are now of limited stability. The cyclopentadienyl-containing cluster **10** reacts with stoichiometric amounts of PPh<sub>3</sub> to give MoIr<sub>3</sub>(μ-CO)<sub>3</sub>(CO)<sub>8-n</sub>(PPh<sub>3</sub>)<sub>n</sub>(η-C<sub>5</sub>H<sub>5</sub>) (*n* = 1, 2), one isomer of the mono-substituted cluster being identified by a structural study [8]. In contrast, the pentamethylcyclopentadienyl-containing **1** reacts with PPh<sub>3</sub> in the present studies to give a bis-substituted cluster only. We have reported extensive studies of <sup>13</sup>CO labelled phosphine derivatives of WIr<sub>3</sub>(CO)<sub>11</sub>(η-C<sub>5</sub>H<sub>5</sub>) which permitted assignment of the structures of the interconverting isomers [4]. The structural study of **5** in the present work has revealed a heretofore unknown ligand disposition for a bis-phosphine derivative in the Group 6–iridium system.

Alkyne chemistry of Group 6–iridium clusters has been the focus of many studies [5,7,10–14], but the

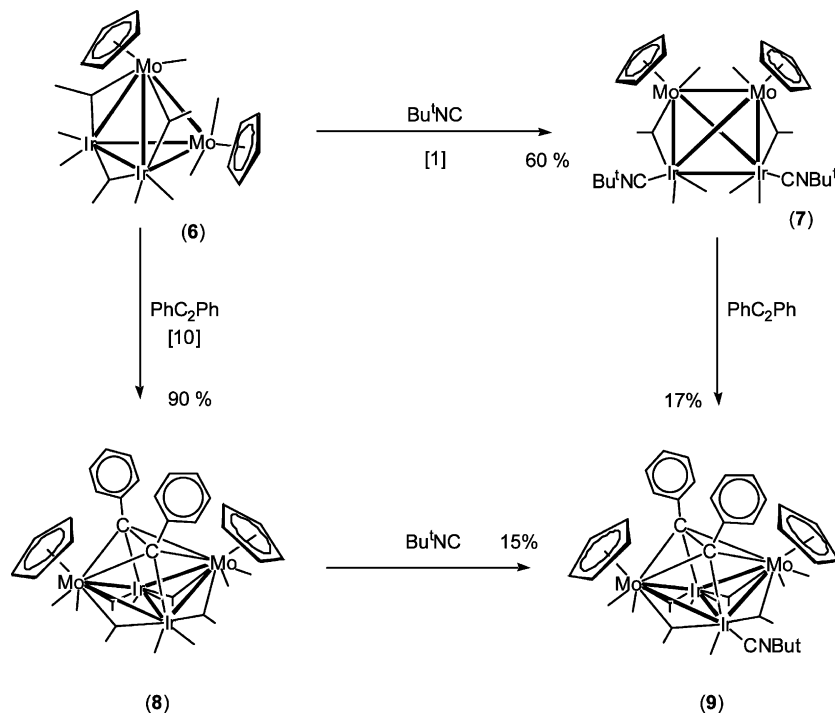
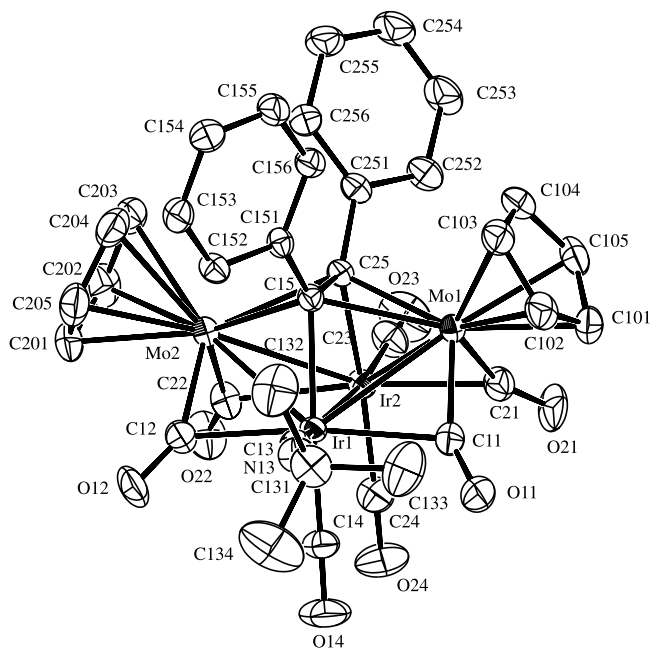
Table 3  
Selected bond lengths (Å) and angles (°) for MoIr<sub>3</sub>(μ-CO)<sub>3</sub>(CO)<sub>6</sub>(PPh<sub>3</sub>)<sub>2</sub>(η-C<sub>5</sub>Me<sub>5</sub>) (**5**)

Bond lengths			
Ir1–Ir2	2.6811(3)	Ir3–C32	1.944(6)
Ir1–Ir3	2.7391(3)	Ir3–C33	1.940(6)
Ir1–Mo4	2.8478(5)	Mo4–C14	2.149(6)
Ir2–Ir3	2.7475(3)	Mo4–C24	2.138(6)
Ir2–Mo4	2.8362(5)	Mo4–C41	1.962(6)
Ir3–Mo4	2.9093(5)	O11–C11	1.119(7)
Ir1–P1	2.3315(13)	O12–C12	1.178(7)
Ir1–C11	1.890(6)	O14–C14	1.185(6)
Ir1–C12	2.126(5)	O21–C21	1.144(7)
Ir1–C14	2.115(5)	O24–C24	1.190(7)
Ir2–P2	2.3343(14)	O31–C31	1.127(7)
Ir2–C12	2.076(6)	O32–C32	1.134(7)
Ir2–C21	1.867(6)	O33–C33	1.118(7)
Ir2–C24	2.119(5)	O41–C41	1.153(7)
Ir3–C31	1.895(6)		
Bond angles			
Ir2–Ir1–Ir3	60.905(7)	Ir1–Mo4–C14	47.59(14)
Ir2–Ir1–Mo4	61.638(11)	Ir2–Mo4–C14	102.38(14)
Ir3–Ir1–Mo4	62.728(11)	Ir2–Mo4–C24	47.92(15)
Ir1–Ir2–Ir3	60.591(7)	Ir1–C11–O11	177.0(5)
Ir1–Ir2–Mo4	62.075(11)	Ir1–C12–O12	138.9(5)
Ir3–Ir2–Mo4	62.780(11)	Ir2–C12–O12	141.7(4)
Ir1–Ir3–Ir2	58.505(7)	Ir1–C14–O14	135.7(4)
Ir1–Ir3–Mo4	60.465(11)	Mo4–C14–O14	140.5(4)
Ir2–Ir3–Mo4	60.10(1)	Ir2–C21–O21	178.0(6)
Ir1–Mo4–Ir3	56.81(1)	Ir2–C24–O24	135.2(4)
Ir2–Mo4–Ir3	57.12(1)	Mo4–C24–O24	141.2(4)
Ir1–Mo4–Ir2	56.29(1)	Ir3–C31–O31	176.8(6)
Ir2–Ir1–C12	49.52(16)	Ir3–C32–O32	176.1(6)
Ir1–Ir2–C12	51.19(15)	Ir3–C33–O33	178.0(5)
Mo4–Ir1–C14	48.61(15)	Mo4–C41–O41	169.5(5)
Mo4–Ir2–C24	48.51(15)		

present study provides the first example of carbonyl replacement at alkyne-containing Group 6–iridium clusters. Reaction of Mo<sub>2</sub>Ir<sub>2</sub>(μ<sub>4</sub>-η<sup>2</sup>-PhC<sub>2</sub>Ph)(μ-CO)<sub>4</sub>(CO)<sub>4</sub>(η-C<sub>5</sub>H<sub>5</sub>)<sub>2</sub> (**8**) with Bu<sup>t</sup>NC proceeds to afford Mo<sub>2</sub>Ir<sub>2</sub>(μ<sub>4</sub>-η<sup>2</sup>-PhC<sub>2</sub>Ph)(μ-CO)<sub>4</sub>(CNBu<sup>t</sup>)(CO)<sub>3</sub>(η-C<sub>5</sub>H<sub>5</sub>)<sub>2</sub> (**9**) in low yield, a structural study revealing substitution at the sterically less-encumbered sites *trans* to the Ir–Ir bond. Reaction of Mo<sub>2</sub>Ir<sub>2</sub>(μ-CO)<sub>2</sub>(CNBu<sup>t</sup>)<sub>2</sub>(CO)<sub>6</sub>(η-C<sub>5</sub>H<sub>5</sub>)<sub>2</sub> (**7**) with diphenylacetylene was assayed as a possible route to a more highly isocyanide-substituted alkyne-containing cluster, but **9** was the only definitively identified product from the complex mixture obtained, indicating loss of isocyanide is competitive with loss of carbonyl in these clusters.

### 3. Experimental

Reactions were performed under an atmosphere of dry dinitrogen (available in-house from liquid nitrogen boiloff) using standard Schlenk techniques [15] although no precautions were taken to exclude air during workup of the cluster products. All reaction solvents used were

Scheme 1. Reactions of  $\text{Mo}_2\text{Ir}_2(\mu\text{-CO})_3(\text{CO})_7(\eta\text{-C}_5\text{H}_5)_2$  (**6**) with  $\text{Bu}^t\text{NC}$  and  $\text{PhC}_2\text{Ph}$ .Fig. 2. ORTEP [9] plot and atomic numbering scheme for  $\text{Mo}_2\text{Ir}_2(\mu_4\text{-}\eta^2\text{-PhC}_2\text{Ph})(\mu\text{-CO})_4(\text{CNBu}^t)(\text{CO})_3(\eta\text{-C}_5\text{H}_5)_2$  (**9**). Displacement ellipsoids are at the 30% probability level. Hydrogen atoms have been omitted for clarity.

analytical reagent (AR) grade.  $\text{CH}_2\text{Cl}_2$  solvent was dried over  $\text{CaH}_2$  and distilled under dry nitrogen using standard methods. Petroleum refers to a petroleum fraction of boiling range 60–80 °C. Pentamethylcyclo-

pentadiene,  $\text{Bu}^t\text{NC}$ , diphenylacetylene and  $\text{PPh}_3$  (Aldrich) were used as received. Literature procedures (or minor modifications thereof) were used to synthesize **1** [16], **6** [17], **7** [1] and **8** [10].

Cluster products were purified by thin-layer chromatography (TLC) on 20 × 20 cm glass plates coated with Merck GF<sub>254</sub> silica gel (0.5 mm). Analytical TLC, used for monitoring the extent of reaction, was carried out on aluminium sheets coated with 0.25 mm silica gel.

Infrared spectra were recorded on a Perkin–Elmer System 2000 FTIR with  $\text{CaF}_2$  solution cells; spectral frequencies are recorded in  $\text{cm}^{-1}$ . All analytical spectra were recorded as solutions in cyclohexane or  $\text{CH}_2\text{Cl}_2$  (AR grade).  $^1\text{H-NMR}$  spectra were recorded in  $\text{CDCl}_3$  (Cambridge Isotope Laboratories) using a Varian Gemini-300 spectrometer (at 300 MHz) and are referenced to the residual non-deuterated  $\text{CHCl}_3$  solvent peak at 7.24 ppm. Secondary ion mass spectra (SIMS) and FABMS were recorded using a VG ZAB 2SEQ instrument (30 kV  $\text{Cs}^+$  ions, current 1 mA, accelerating potential 8 kV, 3-nitrobenzyl alcohol matrix) at the Research School of Chemistry, Australian National University, or the Department of Chemistry, University of Western Australia. All MS were calculated with  $m/z$  based on  $^{96}\text{Mo}$  and  $^{192}\text{Ir}$  assignments, and are reported in the form:  $m/z$  (assignment, relative intensity). Elemental microanalyses were carried out by the Microanalysis Service Unit in the Research School of Chemistry, Australian National University.

Table 4  
Selected bond lengths (Å) and angles (°) for  $\text{Mo}_2\text{Ir}_2(\mu_4\text{-}\eta^2\text{-PhC}_2\text{Ph})(\mu\text{-CO})_4(\text{CNBu}^t)(\text{CO})_3(\eta\text{-C}_5\text{H}_5)_2$  (**9**)

Bond lengths			
Ir1–Ir2	2.6897(3)	Ir2–C22	2.324(6)
Ir1–Mo1	2.7930(5)	Ir2–C23	1.928(7)
Ir1–Mo2	2.8122(5)	Ir2–C24	1.905(7)
Ir2–Mo1	2.8360(5)	Mo1–C11	1.982(7)
Ir2–Mo2	2.8160(5)	Mo1–C21	1.999(6)
Ir1–C15	2.133(5)	Mo2–C12	2.009(6)
Ir2–C25	2.122(5)	Mo2–C22	1.987(7)
Mo1–C15	2.353(5)	O11–C11	1.182(8)
Mo1–C25	2.341(5)	O12–C12	1.179(8)
Mo2–C15	2.329(5)	O14–C14	1.131(8)
Mo2–C25	2.383(5)	O21–C21	1.163(8)
C15–C25	1.475(7)	O22–C22	1.169(8)
Ir1–C11	2.308(6)	O23–C23	1.108(8)
Ir1–C12	2.215(6)	O24–C24	1.134(9)
Ir1–C13	1.991(6)	N13–C13	1.156(8)
Ir1–C14	1.886(6)	N13–C131	1.464(9)
Ir2–C21	2.310(7)		
Bond angles			
Ir1–Ir2–Mo1	60.656(11)	Mo1–C25–Mo2	126.1(2)
Ir1–Ir2–Mo2	61.382(12)	Mo1–C25–C15	72.1(3)
Ir1–Mo2–Ir2	57.095(11)	Mo2–C25–C15	69.8(3)
Ir1–Mo1–Ir2	57.080(11)	Mo2–C15–C25	73.8(3)
Ir2–Ir1–Mo1	62.264(12)	C15–Mo1–C25	36.62(18)
Ir2–Ir1–Mo2	61.523(12)	C15–Mo2–C25	36.45(18)
Mo1–Ir1–Mo2	97.392(15)	Ir1–C11–O11	124.4(5)
Mo1–Ir2–Mo2	96.320(15)	Ir1–C12–O12	126.7(5)
Ir1–C15–Mo1	76.86(16)	Ir1–C13–N13	170.2(6)
Ir1–C15–Mo2	78.02(16)	Ir1–C14–O14	179.4(7)
Ir1–C15–C25	106.7(3)	Ir2–C21–O21	124.4(6)
Ir1–Mo1–C25	68.69(12)	Ir2–C22–O22	124.5(5)
Ir2–Mo1–C25	47.21(13)	Ir2–C23–O23	176.7(7)
Ir2–C25–C15	106.4(3)	Ir2–C24–O24	177.6(8)
Ir2–C25–Mo1	78.74(17)	Mo1–C11–O11	154.5(6)
Ir2–C25–Mo2	77.14(17)	Mo1–C21–O21	153.5(6)
Mo1–C15–C25	71.3(3)	Mo2–C12–O12	149.8(6)
Mo1–C15–Mo2	128.2(2)	Mo2–C22–O22	154.2(6)

### 3.1. Reaction of $\text{MoIr}_3(\mu\text{-CO})_3(\text{CO})_8(\eta\text{-C}_5\text{Me}_5)$ with one equivalent of $\text{Bu}^t\text{NC}$

$\text{Bu}^t\text{NC}$  (4  $\mu\text{l}$ , 0.04 mmol) was added to a light orange solution of **1** (38.0 mg, 0.034 mmol) in  $\text{CH}_2\text{Cl}_2$  (20 ml) and stirred at room temperature (r.t.) for 16 h. The resulting orange solution was reduced to dryness in vacuo, the residue redissolved in a minimum of  $\text{CH}_2\text{Cl}_2$  (ca. 1 ml) and applied to preparative TLC plates. Elution with  $\text{CH}_2\text{Cl}_2$ –petroleum (1/1) gave three bands. The contents of the first band ( $R_f = 0.71$ ) were identified as unreacted **1** (5.4 mg, 0.005 mmol, 15%) by solution IR. The contents of the second band ( $R_f = 0.61$ ) were crystallized from  $\text{CH}_2\text{Cl}_2$ –MeOH to afford dendritic orange crystals identified as  $\text{MoIr}_3(\mu\text{-CO})_3(\text{CNBu}^t)(\text{CO})_7(\eta\text{-C}_5\text{Me}_5)$  (**2**) (21.7 mg, 0.018 mmol, 58%). IR ( $c\text{-C}_6\text{H}_{12}$ ):  $\nu(\text{NC})$  2184m,  $\nu(\text{CO})$  2069s, 2041vs, 2037vs, 2027m, 2012s, 2001m, 1990w, 1986w, 1899w, 1864m, 1847vw, 1810m, 1791w, 1780m

$\text{cm}^{-1}$ .  $^1\text{H-NMR}$  (acetone- $d_6$ ):  $\delta$  1.94 (s, 15H,  $\text{C}_5\text{Me}_5$ ), 1.52 (s, 9H,  $\text{Bu}^t\text{NC}$ ) ppm. MSSI: 1143 ( $[\text{M-CO}]^+$ , 2); 1115 ( $[\text{M-2CO}]^+$ , 22); 1087 ( $[\text{M-3CO}]^+$ , 100); 1059 ( $[\text{M-4CO}]^+$ , 16); 1031 ( $[\text{M-5CO}]^+$ , 41); 1003 ( $[\text{M-6CO}]^+$ , 18); 975 ( $[\text{M-7CO}]^+$ , 26); 947 ( $[\text{M-8CO}]^+$ , 11); 919 ( $[\text{M-9CO}]^+$ , 5); 891 ( $[\text{M-10CO}]^+$ , 8). Anal. Found: C, 25.66; H, 1.92; N, 1.30.  $\text{C}_{25}\text{H}_{24}\text{Ir}_3\text{MoNO}_{10}$ . Calc. C, 25.64; H, 2.07; N, 1.20%. The contents of the third band ( $R_f = 0.47$ ) were purified by vapour diffusion of ether into a  $\text{CH}_2\text{Cl}_2$  solution to afford a light orange powder tentatively identified as  $\text{MoIr}_3(\mu\text{-CO})_3(\text{CNBu}^t)_2(\text{CO})_6(\eta\text{-C}_5\text{Me}_5)$  (**3**) (0.8 mg, 0.0006 mmol, 2%) which decomposed to an uncharacterizable brown solid over days. IR ( $c\text{-C}_6\text{H}_{12}$ ):  $\nu(\text{NC})$  2181m, 2154m,  $\nu(\text{CO})$  2050s, 2024vs, 2007vs, 1998s, 1988s, 1978m, 1881m, 1854m, 1840m, 1801m, 1793sh, 1769s  $\text{cm}^{-1}$ .

### 3.2. Reaction of $\text{MoIr}_3(\mu\text{-CO})_3(\text{CO})_8(\eta\text{-C}_5\text{Me}_5)$ with two equivalents of $\text{Bu}^t\text{NC}$

Following the procedure of Section 3.1,  $\text{Bu}^t\text{NC}$  (8  $\mu\text{l}$ , 0.07 mmol) was added to a light orange solution of **1** (39.0 mg, 0.035 mmol) in  $\text{CH}_2\text{Cl}_2$  (20 ml) and stirred at r.t. for 16 h. The resulting orange solution was reduced to dryness in vacuo, the residue redissolved in a minimum of  $\text{CH}_2\text{Cl}_2$  (ca. 1 ml) and applied to preparative TLC plates. Elution with  $\text{CH}_2\text{Cl}_2$ –petroleum (1/1) gave five bands. The first trace band ( $R_f = 0.72$ ) was tentatively identified as unreacted starting cluster by comparison of  $R_f$  values. The contents of the second band ( $R_f = 0.64$ ) were identified as **2** (12.7 mg, 0.011 mmol, 31%) by solution IR. The contents of the third band ( $R_f = 0.50$ ) were identified as **3** (18.0 mg, 0.015 mmol, 42%) by solution IR. The contents of the fourth band ( $R_f = 0.41$ ) were in trace amounts and could not be isolated. The contents of the fifth band ( $R_f = 0.34$ ) were precipitated from  $\text{CH}_2\text{Cl}_2$ –ether to afford a light orange powder tentatively identified as  $\text{MoIr}_3(\mu\text{-CO})_3(\text{CNBu}^t)_3(\text{CO})_5(\eta\text{-C}_5\text{Me}_5)$  (**4**) (5.8 mg, 0.005 mmol, 13%) which decomposed to an uncharacterizable brown solid over hours. IR ( $c\text{-C}_6\text{H}_{12}$ ):  $\nu(\text{NC})$  2174m, 2152sh, 2136m,  $\nu(\text{CO})$  2024vs, 2015m, 2005vs, 1997m, 1984s, 1975vs, 1967s, 1848w, 1823s, 1771w, 1747s  $\text{cm}^{-1}$ .

### 3.3. Reaction of $\text{MoIr}_3(\mu\text{-CO})_3(\text{CO})_8(\eta\text{-C}_5\text{Me}_5)$ with one equivalent of $\text{PPh}_3$

Following the procedure of Section 3.1,  $\text{PPh}_3$  (9.6 mg, 0.037 mmol) was added to a light orange solution of **1** (41.0 mg, 0.037 mmol) in  $\text{CH}_2\text{Cl}_2$  (20 ml) and stirred at r.t. for 16 h. The resulting pale orange solution was reduced to dryness in vacuo, the residue redissolved in a minimum of  $\text{CH}_2\text{Cl}_2$  (ca. 1 ml) and applied to preparative TLC plates. Elution with  $\text{CH}_2\text{Cl}_2$ –petroleum (3/2) gave two bands. The contents of the first and major

band ( $R_f = 0.88$ ) were identified as unreacted **1** (34.4 mg, 0.031 mmol, 84%) by solution IR. The contents of the second band ( $R_f = 0.72$ ) were crystallized from  $\text{CHCl}_3$ –MeOH to afford orange plate-like crystals identified as  $\text{MoIr}_3(\mu\text{-CO})_3(\text{CO})_6(\text{PPh}_3)_2(\eta\text{-C}_5\text{Me}_5)$  (**5**) (9.0 mg, 0.006 mmol, 30%). IR ( $c\text{-C}_6\text{H}_{12}$ ):  $\nu(\text{CO})$  2059vs, 2041w, 2017m, 2009m, 1996m, 1983vs, 1958m, 1870m, 1820w, 1810w, 1758m, 1734vs  $\text{cm}^{-1}$ .  $^1\text{H-NMR}$  ( $\text{CDCl}_3$ ):  $\delta$  7.66–7.33 (m, 30H,  $\text{C}_6\text{H}_5$ ), 2.03 (s, 15H,  $\text{C}_5\text{Me}_5$ ) ppm. MSFAB: 1584 ( $[\text{M}]^+$ , 50); 1556 ( $[\text{M}-\text{CO}]^+$ , 41); 1528 ( $[\text{M}-2\text{CO}]^+$ , 10); 1500 ( $[\text{M}-3\text{CO}]^+$ , 100); 1472 ( $[\text{M}-4\text{CO}]^+$ , 24); 1444 ( $[\text{M}-5\text{CO}]^+$ , 32); 1416 ( $[\text{M}-6\text{CO}]^+$ , 22); 1388 ( $[\text{M}-7\text{CO}]^+$ , 13). Anal. Found: C, 41.65; H, 2.61.  $\text{C}_{55}\text{H}_{45}\text{Ir}_3\text{MoO}_9\text{P}_2$ . Calc. C, 41.69; H, 2.86%. A crystal suitable for a single-crystal X-ray structural study was grown by diffusion of EtOH into a  $\text{CH}_2\text{Cl}_2$  solution of **5** at 268 K.

#### 3.4. Reaction of $\text{MoIr}_3(\mu\text{-CO})_3(\text{CO})_8(\eta\text{-C}_5\text{Me}_5)$ with half an equivalent of $\text{PPh}_3$

Following the procedure of Section 3.1,  $\text{PPh}_3$  (3.5 mg, 0.014 mmol) was added to a light orange solution of **1** (34.4 mg, 0.031 mmol) in  $\text{CH}_2\text{Cl}_2$  (20 ml) and stirred at r.t. for 16 h. The resulting pale orange solution was reduced to dryness in vacuo, the residue redissolved in a minimum of  $\text{CH}_2\text{Cl}_2$  (ca. 0.5 ml) and applied to preparative TLC plates. Elution with  $\text{CH}_2\text{Cl}_2$ –petroleum (3/2) gave two bands. The contents of the first and major band ( $R_f = 0.88$ ) were identified as unreacted **1** (31.8 mg, 0.029 mmol, 92%) by solution IR. The contents of the second band ( $R_f = 0.72$ ) were identified as **5** (2.9 mg, 0.002 mmol, 28%) by solution IR.

#### 3.5. Reaction of $\text{Mo}_2\text{Ir}_2(\mu\text{-CO})_2(\text{CNBu}^t)_2(\text{CO})_6(\eta\text{-C}_5\text{H}_5)_2$ with diphenylacetylene

Diphenylacetylene (10.3 mg, 0.058 mmol) was added to a deep purple solution of **7** (12.6 mg, 0.011 mmol) in  $\text{CH}_2\text{Cl}_2$  (15 ml) and the resulting solution heated to reflux for 24 h. The resulting dark green solution was reduced to dryness in vacuo, the residue redissolved in a minimum of  $\text{CH}_2\text{Cl}_2$  and applied to preparative TLC plates. Elution with  $\text{CH}_2\text{Cl}_2$ –petroleum (7/3) afforded eight bands. The first, second, fourth, sixth and eighth bands were in trace amounts and could not be isolated. The contents of the third band ( $R_f = 0.50$ ) were identified as unreacted **7** (0.4 mg, 0.0004 mmol, 3%) by solution IR. The contents of the fifth band ( $R_f = 0.39$ ) were crystallized from  $\text{CH}_2\text{Cl}_2$ –MeOH to afford dark green crystals identified as  $\text{Mo}_2\text{Ir}_2(\mu_4\text{-}\eta^2\text{-PhC}_2\text{Ph})(\mu\text{-CO})_4(\text{CNBu}^t)(\text{CO})_3(\eta\text{-C}_5\text{H}_5)_2$  (**9**) (2.3 mg, 0.002 mmol, 17%). A crystal grown by this method was selected for a single-crystal X-ray structural study. IR ( $c\text{-C}_6\text{H}_{12}$ ):  $\nu(\text{NC})$  2175m,  $\nu(\text{CO})$  2054vs, 2018s, 1792s, 1743m  $\text{cm}^{-1}$ .  $^1\text{H-NMR}$  ( $\text{CDCl}_3$ ):  $\delta$  7.14, 7.00 (2  $\times$  m, 2  $\times$  5H,

$\text{C}_6\text{H}_5$ ), 5.28 (s, 2H,  $\text{CH}_2\text{Cl}_2$ ), 4.66 (s, 10H,  $\text{C}_5\text{H}_5$ ), 1.45 (s, 9H,  $\text{Bu}^t\text{NC}$ ) ppm. MSFAB: 1164 ( $[\text{M}]^+$ , 100); 1136 ( $[\text{M}-\text{CO}]^+$ , 16); 1108 ( $[\text{M}-2\text{CO}]^+$ , 19); 1080 ( $[\text{M}-3\text{CO}]^+$ , 82); 1052 ( $[\text{M}-4\text{CO}]^+$ , 32); 1024 ( $[\text{M}-5\text{CO}]^+$ , 18); 996 ( $[\text{M}-6\text{CO}]^+$ , 30); 968 ( $[\text{M}-7\text{CO}]^+$ , 48). Anal. Found: C, 36.07; H, 2.21; N, 1.23.  $\text{C}_{36}\text{H}_{29}\text{Ir}_2\text{Mo}_2\text{NO}_7\cdot\text{CH}_2\text{Cl}_2$ . Calc. C, 35.58; H, 2.50; N, 1.12%. The seventh band (green,  $R_f = 0.20$ ) was found to decompose slowly during development of the chromatography plates. The  $^1\text{H-NMR}$  spectrum suggested that the band contained **9** and  $\text{Mo}_2\text{Ir}_2(\mu_4\text{-}\eta^2\text{-PhC}_2\text{Ph})(\mu\text{-CO})_4(\text{CNBu}^t)_2(\text{CO})_2(\eta\text{-C}_5\text{H}_5)_2$ . The contents of the band were crystallized from  $\text{CH}_2\text{Cl}_2$ –MeOH to afford a brown–green amorphous solid. Purification attempts failed to isolate  $\text{Mo}_2\text{Ir}_2(\mu_4\text{-}\eta^2\text{-PhC}_2\text{Ph})(\mu\text{-CO})_4(\text{CNBu}^t)_2(\text{CO})_2(\eta\text{-C}_5\text{H}_5)_2$  without contamination.

#### 3.6. Reaction of $\text{Mo}_2\text{Ir}_2(\mu_4\text{-}\eta^2\text{-PhC}_2\text{Ph})(\mu\text{-CO})_4(\text{CO})_4(\eta\text{-C}_5\text{H}_5)_2$ with one equivalent of $\text{Bu}^t\text{NC}$

Following the procedure of Section 3.1,  $\text{Bu}^t\text{NC}$  (2  $\mu\text{l}$ , 0.02 mmol) was added to a solution of **8** (21.1 mg, 0.019 mmol) in  $\text{CH}_2\text{Cl}_2$  (10 ml) and stirred at r.t. for 20 h. The dark green solution was reduced to dryness in vacuo, the residue redissolved in a minimum of  $\text{CH}_2\text{Cl}_2$  (ca. 1 ml) and applied to preparative TLC plates. Elution with  $\text{CH}_2\text{Cl}_2$ –petroleum (7/3) afforded three bands. The contents of the first band ( $R_f = 0.47$ ) were identified as unreacted **8** (2.9 mg, 0.003 mmol, 14%) by solution IR. The contents of the second band ( $R_f = 0.34$ ) were identified as  $\text{Mo}_2\text{Ir}_2(\mu_4\text{-}\eta^2\text{-PhC}_2\text{Ph})(\mu\text{-CO})_4(\text{CNBu}^t)(\text{CO})_3(\eta\text{-C}_5\text{H}_5)_2$  (**9**) (3.3 mg, 0.003 mmol, 15%) by solution IR. The contents of the third band were in trace amounts and could not be isolated.

#### 3.7. X-ray crystallographic studies

The crystal and refinement data for compounds **5** and **9** are summarized in Table 2. Crystals suitable for X-ray structural analyses were grown by liquid diffusion techniques from  $\text{CH}_2\text{Cl}_2$ –EtOH at 243 K for **5** and  $\text{CH}_2\text{Cl}_2$ –MeOH at 276 K for **9**. For each study, a single crystal was mounted on a fine glass capillary, and data collected on a Nonius Kappa CCD diffractometer using graphite monochromated Mo– $\text{K}\alpha$  ( $\lambda = 0.71069$  Å). The unit cell parameters were obtained by least squares refinement [18] of  $N_{\text{cell}}$  reflections with  $3 \leq \theta \leq 27^\circ$ . The reduced data [18] were corrected for absorption using numerical methods [19] implemented from within MAXUS [20]; equivalent reflections were merged. The structure of (**5**· $2\text{CH}_2\text{Cl}_2$ ) was solved by direct methods from within the software package SIR92 [21]. The structure (**9**· $\text{CH}_2\text{Cl}_2$ ) was solved by PATTY in DIRDIF [22] implemented from within MAXUS [20].

The crystallographic asymmetric units consist of one molecule of **5** or **9** with two (**5**) or one (**9**) dichloromethane molecules of solvation. All non-hydrogen atoms in **5**·2CH<sub>2</sub>Cl<sub>2</sub> were refined with anisotropic displacement parameters. For **9**·CH<sub>2</sub>Cl<sub>2</sub>, the dichloromethane molecule is disordered over two orientations. Anisotropic displacement parameters were refined for all non-hydrogen atoms except the C and one of the Cl atoms of the disordered dichloromethane solvate. For both structures, H atoms attached to C atoms were included in idealized positions and ride on the atoms to which they are bonded. The final cycles of matrix least squares refinement were based on  $N_{\text{obs}}$  reflections and converged to  $R$  and  $R_w$ . The largest peaks in the final difference electron maps are located near Ir atoms of the cluster (**5**·2CH<sub>2</sub>Cl<sub>2</sub>), or near the Cl atoms of the disordered solvate of (**9**·CH<sub>2</sub>Cl<sub>2</sub>).

#### 4. Supplementary material

Crystallographic data for the structural analyses have been deposited with the Cambridge Crystallographic Data Centre, CCDC nos. 207129 and 207128 for compounds **5** and **9**. Copies of this information may be obtained free of charge from The Director, CCDC, 12 Union Road, Cambridge CB2 1E2, UK (Fax: +44-1223-336033; e-mail: deposit@ccdc.cam.ac.uk or www: <http://www.ccdc.cam.ac.uk>).

#### Acknowledgements

We thank the Australian Research Council (ARC) for financial support and Johnson–Matthey Technology Centre for the generous loan of iridium salts. MGH holds an ARC Australian Senior Research Fellowship and AJU held an ANU Honours Year Scholarship.

#### References

- [1] A.J. Usher, M.G. Humphrey, A.C. Willis, J. Organomet. Chem. 678 (2003) 72 (Part 24).
- [2] S.M. Waterman, N.T. Lucas, M.G. Humphrey, in: A. Hill, R. West (Eds.), Adv. Organomet. Chem., Academic Press, 2000, p. 47.
- [3] J. Lee, M.G. Humphrey, D.C.R. Hockless, B.W. Skelton, A.H. White, Organometallics 12 (1993) 3468.
- [4] S.M. Waterman, M.G. Humphrey, Organometallics 18 (1999) 3116.
- [5] S.M. Waterman, M.G. Humphrey, V.-A. Tolhurst, M.I. Bruce, P.J. Low, D.C.R. Hockless, Organometallics 17 (1998) 5789.
- [6] S.M. Waterman, M.G. Humphrey, D.C.R. Hockless, J. Organomet. Chem. 579 (1999) 75.
- [7] N.T. Lucas, E.G.A. Notaras, S. Petrie, R. Stranger, M.G. Humphrey, Organometallics 22 (2003) 708.
- [8] N.T. Lucas, I.R. Whittall, M.G. Humphrey, D.C.R. Hockless, M.P.S. Perera, M.L. Williams, J. Organomet. Chem. 540 (1997) 147.
- [9] C.K. Johnson, ORTEP-II, A Fortran Thermal Ellipsoid Plot Program, Report ORNL-5138, Oak Ridge National Laboratory, Oak Ridge, Tennessee, USA, 1976.
- [10] N.T. Lucas, M.G. Humphrey, P.C. Healy, M.L. Williams, J. Organomet. Chem. 545–546 (1997) 519.
- [11] N.T. Lucas, M.G. Humphrey, A.D. Rae, Macromolecules 34 (2001) 6188.
- [12] E.G.A. Notaras, N.T. Lucas, J.P. Blitz, M.G. Humphrey, J. Organomet. Chem. 631 (2001) 143.
- [13] N.T. Lucas, E.G.A. Notaras, M.P. Cifuentes, M.G. Humphrey, Organometallics 22 (2003) 284.
- [14] E.G.A. Notaras, N.T. Lucas, M.G. Humphrey, A.C. Willis, A.D. Rae, Organometallics, in press 2003.
- [15] D.F. Shriver, M.A. Drezdson, The Manipulation of Air-sensitive Compounds, Wiley, New York, 1986.
- [16] N.T. Lucas, J.P. Blitz, S. Petrie, R. Stranger, M.G. Humphrey, G.A. Heath, V. Otieno-Alego, J. Am. Chem. Soc. 124 (2002) 5139.
- [17] N.T. Lucas, M.G. Humphrey, D.C.R. Hockless, J. Organomet. Chem. 535 (1997) 175.
- [18] Z. Otwinowski, W. Minor, in: C.W. Carter, Jr., R.M. Sweet (Eds.), Methods in Enzymology, Academic Press, New York, 1997, p. 307.
- [19] P. Coppens, in: F.R. Ahmed, S.R. Hall, C.P. Huber (Eds.), Crystallographic Computing, Munksgaard, Copenhagen, 1970, p. 255.
- [20] S. Mackay, C.J. Gilmore, C. Edwards, N. Stewart, K. Shankland, MAXUS, Computer Program for the Solution and Refinement of Crystal Structures, Nonius, The Netherlands, MacScience, Japan, and The University of Glasgow, UK, 1999.
- [21] A. Altomare, M. Cascarano, C. Giacovazzo, A. Guagliardi, M.C. Burla, G. Polidori, M. Camalli, J. Appl. Cryst. 27 (1994) 425.
- [22] P.T. Beurskens, G. Beurskens, W.P. Bosman, R.S. de Gelder, S. Garcia-Granda, R.O. Gould, J.M.M. Smits, PATTY: The DIRDIF program system, Technical Report of the Crystallography Laboratory, University of Nijmegen, Nijmegen, The Netherlands, 1996.